

CTA-Net: A CNN-Transformer Aggregation Network for Improving Multi-Scale Feature Extraction

Chunlei Meng¹, Jiacheng Yang², Wei Lin¹, Bowen Liu¹, Hongda Zhang¹,
Zhongxue Gan^{1*}, Chun Ouyang^{1*}

¹Fudan University Academy for Engineering and Technology
²Jihua Laboratory

{clmeng23, 22210860047, bwliu22}@m.fudan.edu.cn, {zhanghongda, ganzhongxue, oy_c}@fudan.edu.cn
yangjch@jihualab.ac.cn

Abstract

Convolutional neural networks (CNNs) and vision transformers (ViTs) have become essential in computer vision for local and global feature extraction. However, aggregating these architectures in existing methods often results in inefficiencies. To address this, the CNN-Transformer Aggregation Network (CTA-Net) was developed. CTA-Net combines CNNs and ViTs, with transformers capturing long-range dependencies and CNNs extracting localized features. This integration enables efficient processing of detailed local and broader contextual information. CTA-Net introduces the Light Weight Multi-Scale Feature Fusion Multi-Head Self-Attention (LMF-MHSA) module for effective multi-scale feature integration with reduced parameters. Additionally, the Reverse Reconstruction CNN-Variants (RRCV) module enhances the embedding of CNNs within the transformer architecture. Extensive experiments on small-scale datasets with fewer than 100,000 samples show that CTA-Net achieves superior performance (TOP-1 Acc 86.76%), fewer parameters (20.32M), and greater efficiency (FLOPs 2.83B), making it a highly efficient and lightweight solution for visual tasks on small-scale datasets (fewer than 100,000).

Introduction

Convolutional neural networks (CNNs) have been at the forefront of advancements in computer vision due to their powerful ability to extract detailed, discriminative features (He et al. 2016; Ouyang et al. 2021b,a). By employing convolutional layers, CNNs efficiently capture local spatial hierarchies, contributing to state-of-the-art performance in various image classification tasks. Despite their effectiveness in local feature extraction, the inherent limitation of CNNs lies in the constrained receptive field of small convolutional kernels, which can impede the capture of global contextual information. To address this limitation, researchers often incorporate additional mechanisms or layers to capture a more comprehensive visual context (Ngo et al. 2024; Guo et al. 2022).

Self-attention-based transformers, such as the Vision Transformer (ViT) (Dosovitskiy et al. 2020), have emerged

*These authors contributed equally.

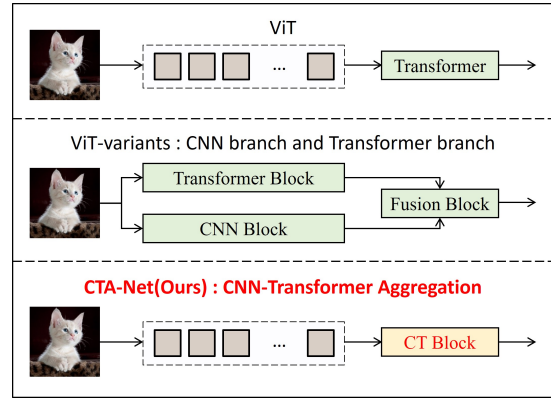


Figure 1: **Top:** ViT use pure Transformer block. **Middle:** The state-of-the-art ViT-Variants use CNN branch and Transformer branch. **Bottom:** CTA-Net use CNN-Transformer Aggregation Network, aggregate CNN into Transformer to take full advantage of the advantages of both.

as a compelling alternative to CNNs, primarily because of their capability to model long-range dependencies. ViT segments an image into patches, transforming them into a sequence of tokens akin to word tokens in natural language processing (NLP). These patches, supplemented by positional embeddings, are fed into stacked transformer blocks to model global relations and extract classification features. The self-attention mechanism, a core component of ViT, enables the network to capture extensive spatial dependencies within images (Yoo et al. 2023).

However, existing transformer-based models (Liang et al. 2021; Chen et al. 2021; Yoo et al. 2023) face challenges in leveraging local and multi-scale features, which are crucial for many visual tasks (Guo et al. 2020b; Mei et al. 2020). Two primary concerns arise when building transformer-based architectures: firstly, although ViT effectively captures long-range dependencies between image patches (Guo et al. 2022), it may neglect the spatial local information within each patch—an area where CNNs excel (Ascoli et al. 2021; Wu et al. 2021). Secondly, the uniform size of tokens in ViT restricts the model’s ability to exploit multi-scale relationships among tokens, which is particularly beneficial for var-

ious downstream tasks (Mei et al. 2020; Shocher, Cohen, and Irani 2018).

Both ViTs and CNNs architectures bring distinct advantages to the table. When integrated effectively, they can leverage their respective strengths to improve model performance (Ngo et al. 2024). While ViT has shown robustness in capturing global representations, particularly with large datasets, it is prone to overfitting on small-scale datasets (fewer than 100,000) due to its reliance on multi-layer perception (MLP) layers (Popescu et al. 2009). Conversely, CNNs are adept at capturing local representations and exhibit robust performance on small-scale datasets but may not scale as efficiently to larger datasets.

This work proposes a new method that integrates the complementary strengths of CNNs and ViTs without increasing unnecessary computation. As illustrated in Figure 1, the proposed CNN-Transformer Aggregation Network (CTA-Net) enhances the capabilities of ViTs by incorporating CNNs as an integral component, compensating for the limitations of pure transformer-based models.

In summary, The main contributions of this paper are as follows:

- The Reverse Reconstruction CNN-Variants (RRCV) module is seamlessly integrated into transformer architectures, combining the local feature extraction capabilities of CNNs with the global contextual understanding of ViTs.
- The Lightweight Multi-Scale Feature Fusion Multi-Head Self-Attention (LMF-MHSA) module efficiently leverages multi-scale features while maintaining a reduced parameter count, enhancing model efficiency and performance, particularly in resource-constrained environments.

Related Works

CNN and Transformer Aggregation Network

The aggregation of CNNs and ViTs has become a key focus in contemporary research (Vasu et al. 2023a), as researchers explore the synergistic combination of CNNs’ local feature extraction capabilities with ViTs’ global contextual understanding (Lu, Sukanuma, and Okatani 2024; Vasu et al. 2023b). Various methods have been developed to blend these strengths, such as the Swin Transformer (Liu et al. 2022), which uses windowed attention mechanisms for implicit local and global feature integration. Other approaches incorporate explicit fusion structures to facilitate the exchange of information between tokens or patches, creating a more unified feature representation (Wu et al. 2021; Guo et al. 2022; Ascoli et al. 2021).

In typical aggregation architectures, CNNs and Transformers are organized into dual branches that independently learn before integration. For example, Dual-ViT (Yao et al. 2023) uses two distinct pathways to capture both global and local information. ECT (Yoo et al. 2023) introduces a Fusion Block to bidirectionally connect intermediate features between CNN and Transformer branches, enhancing the strengths of each. SCT-Net (Xu et al. 2024) proposes a

dual-branch architecture where CNN and Transformer features are aligned to encode rich semantic information and spatial details, which the Transformer utilizes during inference. Crossformer++ (Wang et al. 2023b) extends this concept with a pyramid structure inspired by CNNs to hierarchically expand channel capacity while reducing spatial resolution.

Despite these advances, such architectures often treat CNNs and Transformers as separate modules that interact superficially, necessitating fusion blocks or similar structures to assist feature integration. This separation can hinder information flow between the two, potentially leading to information loss. Moreover, for small-scale datasets where the features for learning are limited, these fusion architectures may restrict comprehensive feature learning (Guo et al. 2022). This limitation is particularly problematic in tasks requiring detailed local features and comprehensive global context, such as image classification.

Multi-Head Self-Attention Mechanism

The Multi-Head Self-Attention (MHSA) mechanism is crucial for capturing global dependencies across spatial positions, significantly enhancing Transformer performance in visual tasks (Guo et al. 2020a). However, many MHSA mechanisms rely on single-scale learning processes, which restrict the model’s capacity to capture multi-scale features (Yan, Wu, and Zhang 2024). This limitation is particularly evident in tasks requiring a nuanced understanding of both global context and local features (Hao et al. 2021a). For instance, single-scale MHSA models often fail to exploit the varying levels of granularity in the data, leading to suboptimal feature representation and impairing performance in tasks such as image classification or object detection (Wang et al. 2023a; Hao et al. 2021b).

Recent advancements aim to address these deficiencies by developing multi-scale MHSA models (Luo et al. 2024). Cross-ViT (Chen, Fan, and Panda 2021) introduces an innovative architecture that encodes and fuses multi-scale features, enhancing the model’s ability to leverage various levels of detail from input data. SBCFormer (Lu, Sukanuma, and Okatani 2024) achieves high accuracy and fast computation on single-board computers by introducing a new attention mechanism.

The LCV model (Ngo et al. 2024) addresses domain adaptation challenges by combining CNNs’ local feature extraction with ViTs’ global context understanding. However, the performance is not ideal when faced with small-scale datasets with limited features.

These complexities underscore the ongoing challenge of designing efficient Transformer architectures that effectively capture multi-scale features without incurring prohibitive computational costs. Addressing this issue remains a critical area of research, particularly for applications involving small-scale datasets where comprehensive feature learning is paramount (Gani, Naseer, and Yaqub 2022).

Method

This section provides a concise overview of the proposed CTA-Net network architecture, followed by a detailed intro-

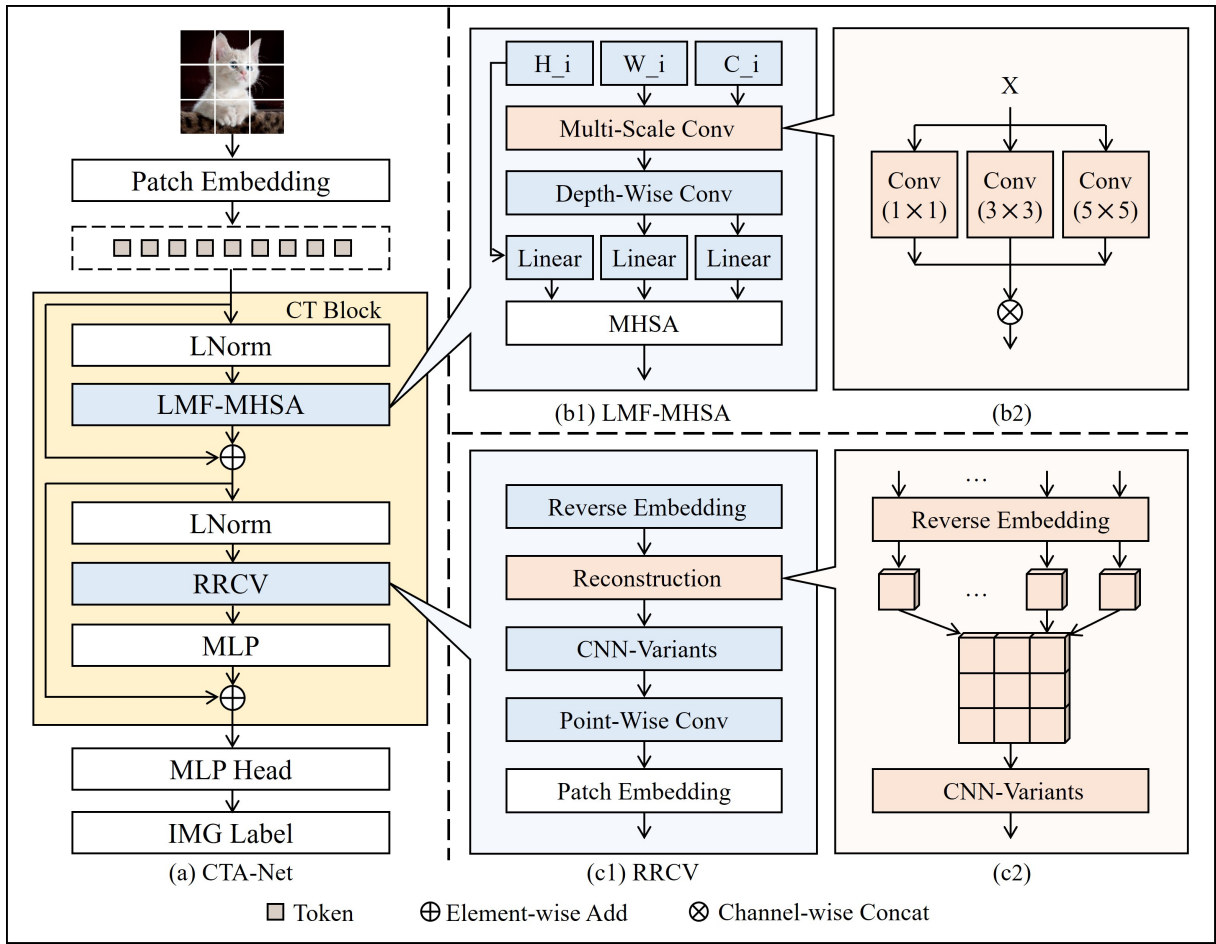


Figure 2: **(a)** illustrates **the overall architecture of CTA-Net**, highlighting the central CNN-Transformer (CT) Block, which integrates CNNs with transformers for enhanced feature extraction. **(b1)** depicts the **LMF-MHSA module**, showcasing the Lightweight Multi-Scale Feature Fusion Multi-Head Self-Attention mechanism, which efficiently learns multi-scale features while reducing computational complexity. **(b2)** provides a detailed view of the **Multi-Scale Conv operation**, demonstrating how different convolution kernel sizes are used to extract multi-scale features from the input. **(c1)** illustrates the **RRCV module**, the Reverse Reconstruction CNN-Variants module, designed to embed CNN operations within the Transformer architecture, leveraging the strengths of both CNNs and transformers. **(c2)** offers a detailed view of the Reconstruction operation process, highlighting how local features extracted by CNNs are seamlessly integrated into the Transformer’s global context.

duction to its components.

Overall Architecture

The intention is to construct an aggregation network that leverages the advantages of both CNNs and Transformers. As illustrated in Figure 2, the CTA-Net is designed to integrate the strengths of CNNs and ViTs. The architecture incorporates two key modules: the RRCV and the LMF-MHSA. These modules ensure a seamless blending of local and global features while maintaining computational efficiency.

In the proposed CTA-Net, the input image is divided into patches, which are transformed into a sequence of tokens. These patches are embedded into a high-dimensional space, similar to the token embedding process in ViTs. Positioned after the initial Layer Normalization (LNorm)

module, the LMF-MHSA module replaces the conventional Multi-Head Self-Attention (MHSA) mechanism, efficiently handling multi-scale feature fusion while reducing computational complexity and memory usage. This is achieved by considering different scales of the input tokens, thereby reducing the computational load compared to traditional MHSA. Located after the second LNorm module and before the Multi-Layer Perceptron (MLP) module in the Transformer block, the RRCV module integrates CNN operations into the Transformer. This module enhances local feature extraction through convolution operations and reconstructs these features to blend with the Transformer’s global context, ensuring the local details captured by CNNs are effectively utilized within the Transformer architecture. The sequence of tokens then passes through multiple Transformer blocks, each consisting of the LMF-MHSA and RRCV mod-

ules, ensuring comprehensive feature extraction at both local and global levels by leveraging the strengths of CNNs and Transformers. Finally, the token representations are fed into a classification head to perform the desired vision task, such as image classification. By fully integrating CNNs and Transformers, CTA-Net effectively captures both local and global features, leading to more comprehensive and accurate feature representation, reduced computational complexity, and improved performance. Extensive experiments on benchmark datasets demonstrate that CTA-Net outperforms existing methods in various vision tasks, providing a robust and practical solution for real-world applications.

Reverse Reconstruction CNN-Variants

CNNs have historically excelled in various computer vision tasks by effectively capturing local features among adjacent pixels. Throughout their evolution, numerous variant architectures have emerged, such as ResNet (He et al. 2016) and depth-wise separable convolutions (Tan and Le 2019). These innovations have addressed specific challenges inherent to deep networks, such as mitigating the degradation problem that arises with increasing depth and reducing the excessive parameterization typically associated with traditional convolutional networks.

The RRCV module’s integration into CTA-Net follows a multi-step process, as illustrated in Figure 2(c1). Initially, a reverse embedding function $RE(\cdot)$ is applied to the Transformer-generated vectors X_T , reconstructing them into feature maps X_{f_map} that align with the input specifications of convolutional neural networks. Subsequently, Point-Wise Convolution ($PC_{onv}(\cdot)$) is utilized to effectively reduce data dimensionality and computational complexity. The final step involves using the patch embedding function $E(\cdot)$ to integrate these processed vectors back into the Transformer framework seamlessly, avoiding the need for an intermediate fusion block that could potentially cause information loss. This process is formally expressed as follows:

$$X_{f_map} = CNN(RE(X_T)) \quad (1)$$

$$X_{RRCV} = E(PC_{onv}(X_{f_map})) \quad (2)$$

Reconstruction As depicted in Figure 2(c2), the reconstruction process is designed to recover the intermediate results of the Transformer into the original feature maps, preserving the corresponding positional information through position embedding combination. These reconstructed feature maps are then processed by our designed CNN-Variants module. Here, $R^{C \times H \times W}$ represents a tensor describing a feature map with dimensions C, H, W and $R^{C \times N \times H_p \times W_p}$ represents a patch with dimensions C, N, H_p, W_p

$$R^{C \times H \times W} = Reconstruct(R^{C \times N \times H_p \times W_p}, H, W) \quad (3)$$

By avoiding the necessity for a distinct fusion block, the proposed architecture facilitates a seamless blending of CNN and ViT components, ensuring that feature extraction and integration occur without the information loss that can

accompany intermediate processing stages. This seamless blending results in a more cohesive and efficient model architecture, effectively harnessing the strengths of both CNN and ViT to achieve superior performance in visual recognition tasks.

CNN-Variants The CNN-Variants module is designed to enhance the ViT’s ability to capture local spatial details, which are otherwise limited due to its patch-based approach. By reconstructing ViT vectors into feature maps, the module enables effective local information extraction, subsequently integrating these features with the ViT’s global context. To validate the effectiveness of local feature extraction, This paper examines three specific variants of CNNs: standard CNN, residual modules, and depth-wise separable convolution modules. The standard CNN serves as a baseline, illustrating the effectiveness of traditional convolutional methods in extracting local features. Residual modules are selected for their ability to mitigate the vanishing gradient problem in deep networks, thereby enhancing the model’s feature learning capacity. Depth-wise separable convolution modules are employed for their efficiency in reducing parameter count while preserving feature extraction accuracy which are critical consideration in resource-constrained environments.

These variants allow for a systematic evaluation of how different convolutional strategies can optimize the integration of local and global features within a Transformer framework.

Light Weight Multi-Scale Feature Fusion Multi-Head Self-Attention

The LMF-MHSA module addresses computational complexity and multi-scale feature extraction challenges in modern computer vision tasks. Traditional MHSA mechanisms are resource-intensive and struggle to capture features across multiple scales, leading to suboptimal object detection. The proposed LMF-MHSA, as shown in Figure 2(b1), significantly reduces computational costs while enhancing feature extraction through a multi-scale fusion mechanism.

Multi-scale Feature Fusion As shown in Figure 2(b2), The multi-scale feature fusion layer is used to extract features at different scales from the input to improve the model’s sensitivity to various scale features. Given an input feature map X , multi-scale features was extracted by using different convolution kernel sizes:

$$X_s = \text{Concat}(\text{Conv}(X_1), \text{Conv}(X_3), \text{Conv}(X_5)) \quad (4)$$

where $X_1, X_3,$ and X_5 represent the feature maps processed by $1 \times 1, 3 \times 3,$ and 5×5 convolution kernels, respectively.

Lightweight Multi-head Self-attention Mechanism The LMF-MHSA mechanism introduces several innovative approaches to enhance computational efficiency while preserving model performance:

Depthwise Separable Convolution. This operation decomposes standard convolutions into depthwise and pointwise steps, significantly reducing the number of parameters and the computational load. A conventional convolutional layer with parameters $M \times N \times D \times D$ is transformed into

a more efficient structure with $M \times D \times D + M \times N$ parameters.

Query, Key, and Value Linear Projections. To optimize resource usage, 1×1 convolutions replace traditional matrix multiplications for transforming the Query, Key, and Value matrices, ensuring data integrity with reduced computational cost.

Attention Computation and Projection. The core attention mechanism is defined by:

$$\text{Attention}(Q, K, V) = \text{Softmax}\left(\frac{QK^T}{\sqrt{d_k}}\right)V$$

where d_k represents the dimensionality of the key. Additional linear projections are applied:

$$K' = \text{Linear}(K)$$

$$V' = \text{Linear}(V)$$

This approach focuses computational efforts on the most pertinent features, balancing precision and efficiency.

Output Features and Efficiency. The LMF-MHSA output is calculated by integrating attention weights with the transformed value vectors:

$$\text{LMF-MHSA}(X) = \text{Attention}(Q, K', V')$$

Through a structured process ranging from initial convolutional refinement to optimized attention calculation the LMF-MHSA mechanism effectively captures both local and global features. This makes it particularly suitable for tasks involving small-scale datasets (fewer than 100,000) and constrained computational resources.

Experiments

This section outlines the comprehensive experiments conducted to assess the effectiveness of the proposed CTA-Net and its individual components. Comparative evaluations were performed on benchmark datasets against SOTA approaches. The datasets and implementation details are presented first, followed by a series of ablation studies to validate the performance of individual modules. Finally, comparative experiments illustrate the superiority of CTA-Net over existing SOTA methods.

Datasets and Implementation Details

Datasets ViT and its variants perform well when pre-trained on large-scale datasets, but tend to perform poorly on small-scale datasets (fewer than 100,000) without such pre-training. In contrast, CNN performs well on small-scale datasets, but ViT tends to perform poorly when dealing with small-scale datasets. To verify that CTA-Net fully exploits the advantages of both architectures, the proposed CTA-Net is evaluated on four small-scale datasets. The four open-source small-scale datasets include CIFAR-10, CIFAR-100 (Krizhevsky, Hinton et al. 2009), APTOS 2019 Blindness Detection (APTOS2019) (Mohanty et al. 2023), and 2020 Retinal Fundus Multi-Disease Image Dataset (RFMiD2020) (Pachade et al. 2021). The dataset details are shown in Appendix A. To enhance the diversity of training data, a series of data augmentation techniques are applied, including random cropping, rotation, horizontal flipping, and color jittering.

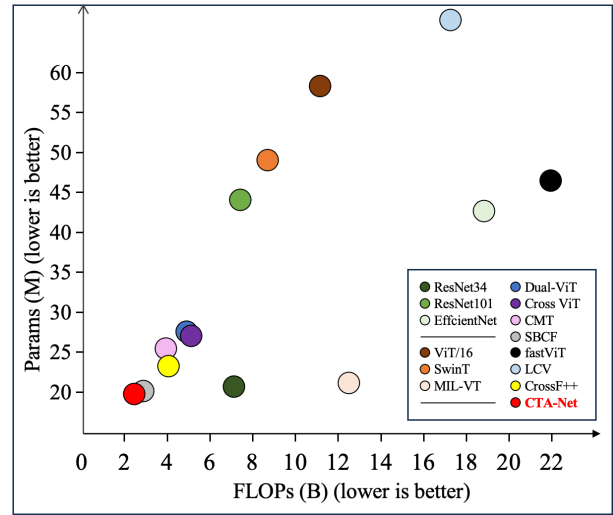


Figure 3: Improvement of CTA-Net over CNN-Variants, ViT-Variants and ViT-Aggregation Model. Circles of different colors represent different models. The closer to the lower left corner, the smaller the model parameters and the higher the efficiency. **The red circle representing CTA-Net is closest to the lower left corner, and the model is the lightest and most efficient.**

Implementation Details The experiments were conducted to evaluate the feature self-learning capabilities of CTA-Net and the integration of CNN and Transformer components without utilizing pre-trained weights. Model performance was assessed using TOP-1 Accuracy (TOP-1 Acc) as a metric of classification accuracy, and computational efficiency was measured in terms of Floating Point Operations per Second (FLOPs) and the number of parameters (Params). All experiments were executed on NVIDIA Tesla A100 GPUs, each equipped with 80 GB of memory.

All experiments were conducted on NVIDIA Tesla A100 GPUs, each with 80 GB of memory.

Comparison with State-Of-The-Art Methods

Table 1 presents the experimental results of CTA-Net on the four small-scale datasets. Compared to other CNN-Variants and ViT-Variants models, CTA-Net demonstrates superior performance. As illustrated in Figure 3, CTA-Net achieves excellent results with the lowest number of parameters and highest efficiency.

Comparisons with CNN-Variants Models. The experimental evaluation involved benchmarking CTA-Net against leading CNN and ViT models on four small-scale datasets, as detailed in Table 1. CTA-Net significantly outperforms several CNN-Variants. Notably, on the APTOS2019 and RFMiD2020 datasets, CTA-Net achieves 3.67% and 5.1% higher TOP-1 accuracy, respectively, than the average of three CNN-Variants. On the RFMiD2020 dataset, CTA-Net surpasses ResNet34 (He et al. 2016) by 9.22%. These results underscore CTA-Net’s enhanced feature learning capabilities, with optimized parameter volume (20.32M) and FLOPs

Type	Model	Reference	APTOS 2019	RFMiD 2020	CIFAR 10	CIFAR 100	FLOPs (B)	Params (M)
CNN-Variants	ResNet34	CVPR 2016	73.22%	72.81%	60.74%	33.75%	7.34	21.29
	ResNet101	ICLR 2016	70.77%	80%	68.22%	40.10%	7.80	44.60
	EfficientNet	IMCL 2019	75.68%	77.97%	65.91%	36.58%	19	43
ViT-Variants	ViT/16	ICLR 2020	64.21%	80.62%	67.42%	41.41%	11.28	57.96
	SwinT	CVPR 2022	68.3%	81.1%	79.3%	63.59%	8.70	49.56
	MIL-VT	MICCAI 2021	61.95%	72.8%	49%	34.5%	12.52	21.72
ViT-Aggregation	Dual-ViT	TPAMI 2023	70.77%	80.63%	86.94%	-	5.40	27.59
	Cross ViT	ICCV 2021	69.13%	80.01%	75%	49.94%	5.60	26.79
	CMT	CVPR 2022	76.77%	80.61%	-	-	4	25.10
	SBCF	WACV 2024	71.3%	80.62%	-	-	2.91	20.68
	fastViT	ICCV 2023	74.72%	79.37%	84.72%	59.2%	22	46
	LCV	CVPR 2024	72.95%	80.66%	-	-	16.86	86.98
	CrossF++	TPAMI 2023	47%	79.38%	80.49%	-	4.08	23.33
	CTA-Net	Ours	76.9%	82.03%	86.76%	59.43%	2.83	20.32

Table 1: Comparison with State-Of-The-Art Methods on small-scale datasets (fewer than 100,000) (Metric:TOP-1 Acc)

(2.83B), making it more efficient than traditional CNN architectures.

Comparisons with ViT-Variants Models. As shown in Table 1, When compared to SOTA ViT models, CTA-Net exhibits remarkable performance, with an average increase in TOP-1 Acc of 12.07%, 3.856%, 21.52%, and 12.93% across the four datasets. On the CIFAR-10 and CIFAR-100 datasets, CTA-Net’s accuracy exceeds MIL-VT (Yu et al. 2021) by 37.76% and 24.93%, respectively, without the reliance on large-scale pre-trained weights. While CTA-Net’s TOP-1 Acc on the CIFAR-100 dataset is slightly lower than SwinT’s, it compensates with significantly reduced FLOPs (5.87B less) and fewer parameters (29.24M less), achieving efficiency four times greater than SwinT (Liu et al. 2022). These results emphasize CTA-Net’s balanced approach, leveraging CNN and ViT advantages to achieve high performance with fewer parameters and enhanced efficiency.

Comparisons with ViT-Aggregation Models. Table 1 presents a comparison between CTA-Net and various ViT-Aggregation models. CTA-Net’s superiority over ViT-Aggregation models is evident, with a 1.652% average improvement in TOP-1 accuracy on small-scale datasets. It was found that fastViT converges very slowly. The TOP-1 Acc on the four small-scale datasets in Table 1 was achieved after training for 350 epochs, while other models were only trained for 100 epochs. The CTA-Net model converges faster and achieves higher performance within the same training cycles, even with limited data, showcasing its robust feature learning capabilities. Although Dual-ViT (Yao et al. 2023) slightly outperforms CTA-Net by 0.18% in TOP-1 accuracy on CIFAR-10, CTA-Net demonstrates a 47.59% higher efficiency and a 26.42% reduction in parameters, which is crucial for resource-constrained environments. Similarly, while CrossF++/s (Wang et al. 2023b) achieves 90% TOP-1 accuracy on CIFAR-10 with multi-epoch training, it requires significantly more computational resources, which conflicts with the practical need for balancing performance

and efficiency. Additionally, It was observed that complex network structures like LCV (Ngo et al. 2024) encounter challenges on the small-scale CIFAR-10 dataset, achieving only 10% TOP-1 accuracy without large-scale pre-trained weights (Not shown in Table 1). This points to the model’s struggle in learning features from limited data.

In comparison to other aggregation models, CTA-Net not only delivers superior performance but also maintains the lowest parameter count (20.32M) and FLOPs (2.83B) among all baselines. This efficiency in feature learning and model deployment makes CTA-Net a compelling choice for applications involving small-scale datasets, improving Multi-Scale feature extraction and addressing the challenges of aggregation CNN and ViT architectures.

Ablation Study

To validate the effectiveness of CTA-Net, a series of ablation studies were conducted, focusing on the key innovative modules: the RRCV module and the LMF-MHSA module. The objective was to demonstrate how each component enhances the overall architecture’s performance and identify the optimal configurations for integrating CNN and Transformer components.

Model	APTOS 2019	RFMiD 2020	CIFAR 10	CIFAR 100
ViT	64.21%	80.62%	67.42%	41.41%
+RRCV	76.36%	80.78%	82.1%	55.73%
+LMF-MHSA	76.9%	82.03%	86.76%	59.43%

Table 2: Effectiveness of the Key Innovative Modules. Metric is TOP-1 Acc. The first row indicates the use of a common vit model, the second row indicates the addition of our proposed RRCV module to this model, and the third row indicates the addition of our proposed LMF-MHSA module to the second row to form CTA-Net.

Effectiveness of the Key Innovative Modules. As depicted in Table 2, the RRCV and LMF-MHSA modules were incrementally added to the baseline to showcase their effectiveness. The addition of the RRCV module increased the TOP-1 Acc on the small-scale datasets by an average of 6.115%, indicating that the RRCV module effectively integrates CNN’s advantages and addresses ViT’s performance limitations on small-scale datasets. Further, incorporating the LMF-MHSA module resulted in an additional average TOP-1 Acc increase of 1.74% across the four datasets, with a minimal increase in FLOPs from 2.48B to 2.83B. This showcases LMF-MHSA’s efficiency in handling multi-scale features.

CNN-Variants	APTOS 2019	RFMiD 2020	CIFAR 10	CIFAR 100
CNN	74.18%	80.62%	82.76%	53.4%
D-W Conv	76.09%	81.25%	76.56%	49.6%
ResNet	76.9%	82.03%	86.76%	59.43%

Table 3: **Comparison on different CNN-Variants of RRCV Module**, Metric is TOP-1 Acc. D-W Conv refers to Depth-Wise Convolution.

Comparison on different CNN-Variants. The RRCV module embeds CNN operations within the Transformer architecture to enhance local feature extraction. Various configurations were tested, as shown in Table 3. Residual convolutions provided the best integration with the Transformer, maximizing performance, as detailed in Appendix B. This suggests that residual connections, which maintain gradient flow and support deeper models, are particularly beneficial for local feature extraction.

Module	FLOPs	Params
MHSA	11.28 B	59.76 M
LMF-MHSA	2.83 B	20.32 M

Table 4: Comparison between the LMF-MHSA module and the MHSA module in terms of model parameters and model efficiency.

Effectiveness of the Light Weight Multi-Scale Feature Fusion Multi-Head Self-Attention Module. The LMF-MHSA module was specifically designed to address parameter and computational efficiency. Table 4 compares the traditional MHSA and LMF-MHSA under identical configurations. The LMF-MHSA module demonstrates a significant reduction in total parameter count to 20.83M, reducing the model complexity by 66%. The model efficiency is increased to 2.83B, an increase of 79.42%. showcasing its ability to maintain model performance while minimizing resource consumption. This efficiency highlights the module’s role in lightweight architecture design, facilitating its application in environments with limited computational capabilities.

Module	APTOS 2019	RFMiD 2020	CIFAR 10	CIFAR 100
1SSC	74.46%	82.03%	84.2%	58.84%
3SSC	73.91%	81.09%	84.89%	58.40%
5SSC	74.18%	81.25%	85.27%	58.94%
MSC	76.9%	82.03%	86.76%	59.43%

Table 5: **Signle-Scale Conv vs. Multi-Scale Conv**, Metric is TOP-1 Acc. 1SSC refers to 1×1 Signle-Scale Conv. 3SSC refers to 3×3 Signle-Scale Conv. 5SSC refers to 5×5 Signle-Scale Conv. MSC refers to Multi-Scale Conv.

The Necessity of Multi-Scale Convolution. The LMF-MHSA module employs multi-scale convolutions to significantly refine the feature extraction process. By enabling the network to capture information across varying levels of granularity, this approach is particularly effective for tasks requiring the recognition of intricate visual patterns. As demonstrated in Table 5, Experiments were conducted with different convolutional kernel sizes to validate the significance of multi-scale convolutions. Several attempts were made to experiment with single-scale convolution. For detailed experiments, refer to Appendix C. The results reveal that combining various kernel sizes in multi-scale convolutions yields an average performance improvement of 1.765% over single-scale convolutions on small-scale datasets. This evidence underscores the critical role of multi-scale feature extraction in enhancing the model’s ability to generalize across diverse visual patterns. The integration of multiple convolutional kernels within the LMF-MHSA module facilitates a more robust feature representation, thereby boosting the overall performance of the CTA-Net architecture.

Conclusion

This paper presents CTA-Net, a CNN-Transformer aggregation network for improving multi-scale feature extraction on small-scale datasets (fewer than 100,000). CTA-Net addresses the challenges of inadequate fusion of CNN and ViT features and high model complexity. By integrating CNN operations within the ViT framework, CTA-Net leverages the strengths of both architectures to enhance local feature extraction and global information processing, improving the network’s representation capabilities. The Reverse Reconstruction CNN Variant (RRCV) and Lightweight Multi-Scale Feature Fusion Multi-Head Self-Attention (LMF-MHSA) modules were validated through extensive ablation experiments. The results demonstrate that CTA-Net achieves a superior TOP-1 Acc of 86.76% over the baseline, with higher efficiency (FLOPs 2.83B) and lower complexity (Params 20.32M). CTA-Net is a suitable aggregation network for small-scale datasets (fewer than 100,000), advancing visual tasks and providing a scalable solution for future recognition research and applications.

References

- Ascoli, S.; Touvron, H.; Leavitt, M. L.; Morcos, A. S.; Biroli, G.; and Sagun, L. 2021. Convit: Improving vision transformers with soft convolutional inductive biases. In *International conference on machine learning*, 2286–2296.
- Chen, C. R.; Fan, Q.; and Panda, R. 2021. Crossvit: Cross-attention multi-scale vision transformer for image classification. In *Proceedings of the IEEE/CVF international conference on computer vision*, 357–366.
- Chen, H.; Wang, Y.; Guo, T.; Xu, C.; Deng, Y.; Liu, Z.; Ma, S.; Xu, C.; Xu, C.; and Gao, W. 2021. Pre-trained image processing transformer. In *Proceedings of the IEEE/CVF conference on computer vision and pattern recognition*, 12299–12310.
- Dosovitskiy, A.; Beyer, L.; Kolesnikov, A.; Weissenborn, D.; Zhai, X.; Unterthiner, T.; Dehghani, M.; Minderer, M.; Heigold, G.; Gelly, S.; et al. 2020. An image is worth 16x16 words: Transformers for image recognition at scale. In *Proceedings of the International Conference on Learning Representations*.
- Gani, H.; Naseer, M.; and Yaqub, M. 2022. How to Train Vision Transformer on Small-scale Datasets? In *Proceedings of the British Machine Vision Conference*.
- Guo, J.; Han, K.; Wu, H.; Tang, Y.; Chen, X.; Wang, Y.; and Xu, C. 2022. Cmt: Convolutional neural networks meet vision transformers. In *Proceedings of the IEEE/CVF conference on computer vision and pattern recognition*, 12175–12185.
- Guo, Q.; Qiu, X.; Liu, P.; Xue, X.; and Zhang, Z. 2020a. Multi-scale self-attention for text classification. In *Proceedings of the AAAI conference on artificial intelligence*, 7847–7854.
- Guo, Y.; Chen, J.; Wang, J.; Chen, Q.; Cao, J.; Deng, Z.; Xu, Y.; and Tan, M. 2020b. Closed-loop matters: Dual regression networks for single image super-resolution. In *Proceedings of the IEEE/CVF conference on computer vision and pattern recognition*, 5407–5416.
- Hao, Y.; Dong, L.; Wei, F.; and Xu, K. 2021a. Self-attention attribution: Interpreting information interactions inside transformer. In *Proceedings of the AAAI Conference on Artificial Intelligence*, 12963–12971.
- Hao, Y.; Dong, L.; Wei, F.; and Xu, K. 2021b. Self-attention attribution: Interpreting information interactions inside transformer. In *Proceedings of the AAAI Conference on Artificial Intelligence*, 12963–12971.
- He, K.; Zhang, X.; Ren, S.; and Sun, J. 2016. Deep residual learning for image recognition. In *Proceedings of the IEEE conference on computer vision and pattern recognition*, 770–778.
- Krizhevsky, A.; Hinton, G.; et al., eds. 2009. *Learning multiple layers of features from tiny images*. Toronto, ON, Canada.
- Liang, J.; Cao, J.; Sun, G.; Zhang, K.; Van Gool, L.; and Timofte, R. 2021. Swinir: Image restoration using swin transformer. In *Proceedings of the IEEE/CVF international conference on computer vision*, 1833–1844.
- Liu, Z.; Ning, J.; Cao, Y.; Wei, Y.; Zhang, Z.; Lin, S.; and Hu, H. 2022. Video swin transformer. In *Proceedings of the IEEE/CVF conference on computer vision and pattern recognition*, 3202–3211.
- Lu, X.; Suganuma, M.; and Okatani, T. 2024. SBCFormer: Lightweight Network Capable of Full-size ImageNet Classification at 1 FPS on Single Board Computers. In *Proceedings of the IEEE/CVF Winter Conference on Applications of Computer Vision*, 1123–1133.
- Luo, F.; Chen, X.; Gong, X.; Wu, W.; and Guo, T. 2024. Dual-Window Multiscale Transformer for Hyperspectral Snapshot Compressive Imaging. In *Proceedings of the AAAI Conference on Artificial Intelligence*, 3972–3980.
- Mei, Y.; Fan, Y.; Zhou, Y.; Huang, L.; Huang, T. S.; and Shi, H. 2020. Image super-resolution with cross-scale non-local attention and exhaustive self-exemplars mining. In *Proceedings of the IEEE/CVF conference on computer vision and pattern recognition*, 5690–5699.
- Mohanty, C.; Mahapatra, S.; Acharya, B.; Kokkoras, F.; Gerogiannis, V. C.; Karamitsos, I.; and Kanavos, A. 2023. Using deep learning architectures for detection and classification of diabetic retinopathy. *Sensors*, 23(12).
- Ngo, B. H.; DoTran, N.; Nguyen, T.; Jeon, H.; and Choi, T. J. 2024. Learning CNN on ViT: A Hybrid Model to Explicitly Class-specific Boundaries for Domain Adaptation. In *Proceedings of the IEEE/CVF Conference on Computer Vision and Pattern Recognition*, 28545–28554.
- Ouyang, C.; Gan, Z.; Zhen, J.; Guan, Y.; Zhu, X.; and Zhou, P. 2021a. Inter-patient classification with encoded peripheral pulse series and multi-task fusion cnn: application in type 2 diabetes. *IEEE Journal of Biomedical and Health Informatics*, 25(8): 3130–3140.
- Ouyang, C.; Zhen, J.; Zhou, P.; Guan, Y.; Zhu, X.; and Gan, Z. 2021b. Peripheral pulse multi-Gaussian decomposition using a modified artificial bee colony algorithm. *Biomedical Signal Processing and Control*, 65: 102319.
- Pachade, S.; Porwal, P.; Thulkar, D.; Kokare, M.; Deshmukh, G.; Sahasrabudde, V.; Giancardo, L.; Quelled, G.; and Mériaudeau, F. 2021. Retinal fundus multi-disease image dataset (RFMiD): a dataset for multi-disease detection research. *Data*, 6(2).
- Popescu, M.-C.; Balas, V. E.; PerescuPopescu, L.; and Matorakis, N. 2009. Multilayer perceptron and neural networks. *WSEAS Transactions on Circuits and Systems*, 8: 579–588.
- Shocher, A.; Cohen, N.; and Irani, M. 2018. “zero-shot” super-resolution using deep internal learning. In *Proceedings of the IEEE conference on computer vision and pattern recognition*, 3118–3126.
- Tan, M.; and Le, Q. 2019. Efficientnet: Rethinking model scaling for convolutional neural networks. In *Proceedings of the International conference on machine learning*.
- Vasu, P. K. A.; Gabriel, J.; Zhu, J.; Tuzel, O.; and Ranjan, A. 2023a. FastViT: A fast hybrid vision transformer using structural reparameterization. In *Proceedings of the IEEE/CVF International Conference on Computer Vision*.

Vasu, P. K. A.; Gabriel, J.; Zhu, J.; Tuzel, O.; and Ranjan, A. 2023b. FastViT: A fast hybrid vision transformer using structural reparameterization. In *Proceedings of the IEEE/CVF International Conference on Computer Vision*, 5785–5795.

Wang, T.; Zhang, K.; Shen, T.; Luo, W.; Stenger, B.; and Lu, T. 2023a. Ultra-high-definition low-light image enhancement: A benchmark and transformer-based method. In *Proceedings of the AAAI Conference on Artificial Intelligence*, 2654–2662.

Wang, W.; Chen, W.; Qiu, Q.; Chen, L.; Wu, B.; Lin, B.; He, X.; and Liu, W. 2023b. Crossformer++: A versatile vision transformer hinging on cross-scale attention. *IEEE Transactions on Pattern Analysis and Machine Intelligence*.

Wu, H.; Xiao, B.; Codella, N.; Liu, M.; Dai, X.; Yuan, L.; and Zhang, L. 2021. Cvt: Introducing convolutions to vision transformers. In *Proceedings of the IEEE/CVF international conference on computer vision*, 22–31.

Xu, Z.; Wu, D.; Yu, C.; Chu, X.; Sang, N.; and Gao, C. 2024. SCTNet: Single-Branch CNN with Transformer Semantic Information for Real-Time Segmentation. In *Proceedings of the AAAI Conference on Artificial Intelligence*, 6378–6386.

Yan, H.; Wu, M.; and Zhang, C. 2024. Multi-Scale Representations by Varying Window Attention for Semantic Segmentation. *arXiv preprint arXiv:2404.16573*.

Yao, T.; Li, Y.; Pan, Y.; Wang, Y.; Zhang, X.-P.; and Mei, T. 2023. Dual vision transformer. *IEEE transactions on pattern analysis and machine intelligence*, 45(9): 10870–10882.

Yoo, J.; Kim, T.; Lee, S.; Kim, S. H.; Lee, H.; and Kim, T. H. 2023. Enriched cnn-transformer feature aggregation networks for super-resolution. In *Proceedings of the IEEE/CVF winter conference on applications of computer vision*, 4956–4965.

Yu, S.; Ma, K.; Bi, Q.; Bian, C.; Ning, M.; He, N.; Li, Y.; Liu, H.; and Zheng, Y. 2021. Mil-vt: Multiple instance learning enhanced vision transformer for fundus image classification. In *Proceedings of the Medical Image Computing and Computer Assisted Intervention*.